Chapter 4
Resistive Bolometers

4.1 Introduction

A bolometer is a temperature-sensitive electrical resistor. Its operation is based on its temperature rise caused by absorption of incident radiant energy. The change in temperature causes a change in electrical resistance, which is measured by an external electrical circuit. When the radiation is removed, the temperature of the bolometer returns to its initial value, which is determined by the ambient surroundings in which it is immersed. If the resistance increases with increasing temperature, such as is found with metals, the bolometer is said to have a positive temperature coefficient of resistance; if it decreases with increasing temperature, as is found in semiconductors under most operating conditions, it is said to have a negative temperature coefficient of resistance.

Modern bolometer arrays employ a pixel structure originally developed by Honeywell, Inc. (see Fig. 4-1). It is termed a monolithic structure and is prepared by silicon micromachining. The detecting area is defined by a thin membrane, usually made of silicon nitride (Si_3N_4), upon which is deposited a thin film of the detecting material, which is usually semiconducting vanadium oxide (VO_x). The membrane is supported above a silicon substrate by means of "legs" made of silicon nitride upon which is an electrically conductive film. The preparation of this structure employs a sacrificial layer of silicon dioxide, later removed, the thickness of which determines the height of the membrane above the substrate. A reflective layer on the substrate below the membrane causes incident infrared radiation that is not completely absorbed by the detecting material to be reflected back through the material, thereby increasing the amount absorbed. This is most effective when the spacing between the absorbing layer and the reflecting layer is one-fourth of the wavelength of the incident radiation. Assuming the incident radiation wavelengths are in the 8–12-μm spectral interval, the spacing is 2.5 μm.

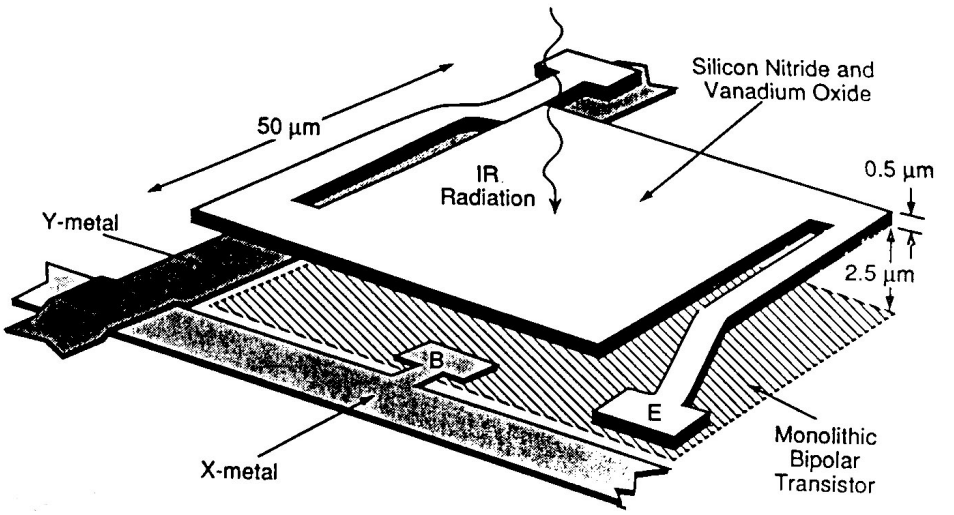

Figure 4-1. Microbolometer pixel structure. From R.A. Wood.[2]

4.2 Responsivity

A complete and accurate representation of a resistive bolometer pixel is a complex and difficult task. It is also hard to fully grasp the influence and interaction of the various parameters. The analysis below attempts to clarify the operation by describing three cases of increasing complexity.

4.2.1 Case I: No Joulean heating; constant bias

Two inputs to the bolometer model are the heat flow equation and the nature of the electrical bias, whether continuous or pulsed. The simplest model, which is widely used, assumes a heat flow equation that omits the Joulean heating of the bias current and also assumes a constant (as opposed to pulsed) electrical bias. This model computes the temperature difference between the silicon substrate and the thermally isolated, radiatively heated, resistive thin film deposited upon a membrane. Heat flows down legs supporting the membrane.

The heat flow equation in this case is that already presented for thermoelectric detectors in Eqs. (3.1) through (3.4). The signal voltage V_s, however, is given by

$$V_s = i_b \alpha R \Delta T \; ; \tag{4.1}$$

where R is the electrical resistance, i_b is the bias current, and α, the temperature coefficient of resistance, is given by

$$\alpha \equiv \frac{1}{R}\frac{dR}{dT}. \tag{4.2}$$

The thermal response time τ_T is the same as for thermoelectric detectors, i.e.,

$$\tau_T = \frac{C}{G}. \tag{3.3}$$

The responsivity $\Re$ is obtained by combining the expression for the temperature rise, Eq. (3.2), with that for the signal voltage, Eq. (4.1), then dividing through by the incident radiant power $P_o A_o$, resulting in

$$\Re = \frac{\eta\beta i_b \alpha R}{G(1+\omega^2\tau_T^2)^{1/2}}; \tag{4.3}$$

The dc responsivity is determined by setting ω=0. It is

$$\Re(\omega = 0) = \frac{\eta\beta i_b \alpha R}{G}. \tag{4.4}$$

Note that the responsivity is inversely proportional to the thermal conductance, which was also true for thermoelectric arrays, see Eq. (3.7).

4.2.2 Case II: Joulean heating; constant bias[1]

An increased complexity is introduced when the heat flow equation includes the Joulean heating due to the electrical bias. Furthermore, a load resistor is introduced into the simple circuit (battery, bolometer, load resistor) in order to distinguish between voltage source operation ($R_L >> R_B$, where R_L is the load resisitance and R_B is the bolometer resistance) and current source operation ($R_L << R_B$), see Fig. 4-2.

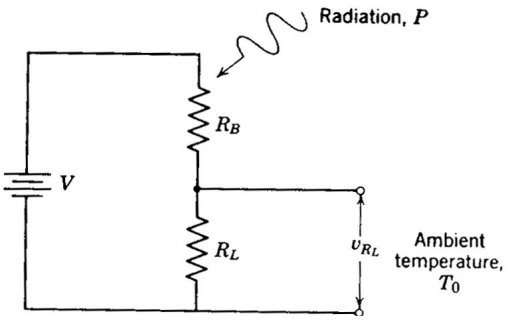

Figure 4-2. Bolometer circuit.

The bolometer is in series with R_L, the load resistor, and the bias supply of voltage V. If the circuit is opened so that no current flows, and if no signal radiation is present, the bolometer is at the ambient temperature T_o. Closing the circuit causes current to flow, such that the Joulean heating in the bolometer element R_B increases its temperature to T_1. At the same time its resistance changes to a value characteristic of that at T_1. If radiation now falls upon the bolometer, its temperature changes by ΔT to the new value T. This results in a resistance change in the bolometer, causing a change in the voltage appearing across R_L.

The dynamic analysis of the operation is based on use of the heat transfer equation for the bolometer. In the absence of radiation, but with current flowing in the circuit, the equation is

$$C\frac{dT}{dt} + G_o(T_1 - T_o) = i^2 R_B \,. \tag{4.5}$$

The first term in Eq. (4.5) represents the influence of the heat capacity C on the rate of change of bolometer temperature, and is zero in the steady state condition. The second term represents heat conduction from the bolometer at temperature T_1 to its surroundings at T_o through a medium of average thermal conductance G_o. In most cases this conduction will be to the substrate, although in ideal operation it represents only radiation interchange with the surroundings. In the latter case, G_o will be a function of T. The term on the right is the Joulean heating of the bolometer.

In the presence of signal radiation such that P_o W per unit area are incident upon it, the bolometer changes its temperature to T by the incremental amount ΔT. The heat transfer equation becomes

$$C\frac{d(\Delta T)}{dt} + G(\Delta T) = \frac{d(i^2 R_B)}{dT}\Delta T + \eta\beta A_D P_o \exp(j\omega t) \,. \tag{4.6}$$

Here G is the thermal conductance when the bolometer pixel is at temperature T, A_D is the pixel area, η is the optical absorption coefficient, β is the fill factor, P_o is the amplitude of the incident radiation power density which is modulated at angular frequency ω, and $j \equiv \sqrt{-1}$. The first term on the right is

$$\frac{d(i^2 R_B)}{dT}\Delta T = \frac{d}{dT}\left[\frac{V^2 R_B}{(R_B + R_L)^2}\right]\Delta T = \frac{V^2(R_L - R_B)}{(R_L + R_B)^3}\frac{dR_B}{dT}\Delta T \,. \tag{4.7}$$

The quantity α describing the dependence of bolometer resistance upon temperature is defined as

$$\alpha \equiv \frac{1}{R_B}\frac{dR_B}{dT}. \tag{4.8}$$

For a semiconductor at room temperature, R_B is approximated by

$$R_B = R_{B0}\exp(b/T). \tag{4.9}$$

Thus, for a semiconductor at room temperature,

$$\alpha = -b/T^2. \tag{4.10}$$

For a metal that has a linear dependence of resistance on temperature, that is,

$$R_B = R_{B0}[1+\gamma(T-T_o)], \tag{4.11}$$

α is given by

$$\alpha = \frac{\gamma}{1+\gamma(T-T_o)}. \tag{4.12}$$

Introducing Eqs. (4.7) and (4.8) into (4.6) results in

$$C\frac{d(\Delta T)}{dt} + G\Delta T = \frac{V^2 R_B \alpha}{(R_L+R_B)^2}\left(\frac{R_L-R_B}{R_L+R_B}\right)\Delta T + \eta\beta A_D P_o \exp(j\omega t). \tag{4.13}$$

However, the Joulean heating in the bolometer in the steady state is related to the thermal conduction losses by

$$\frac{V^2 R_B}{(R_L+R_B)^2} = G_o(T_1 - T_0). \tag{4.14}$$

Therefore, Eq. (4.13) becomes

$$C\frac{d(\Delta T)}{dt} + G_e\Delta T = \eta\beta A_D P_o \exp(j\omega t); \tag{4.15}$$

where G_e, which is referred to as the "effective G," is defined as

$$G_e \equiv G - G_o(T_1 - T_0)\alpha\left(\frac{R_L-R_B}{R_L+R_B}\right). \tag{4.16}$$

The solution to Eq. (4.15) is

$$\Delta T = \Delta T_o \exp\left(-\frac{G_e}{C}t\right) + \frac{\eta\beta A_D P_o \exp(j\omega t)}{G_e + j\omega C}. \tag{4.17}$$

The first term in Eq. (4.17) represents a transient, whereas the second is a periodic function. If G_e is positive, i.e., if

$$G > G_o(T_1 - T_0)\alpha\left(\frac{R_L - R_B}{R_L + R_B}\right), \tag{4.18}$$

then the transient term goes to zero with time and only the periodic function remains. However, if

$$G < G_o(T_1 - T_0)\alpha\left(\frac{R_L - R_B}{R_L + R_B}\right), \tag{4.19}$$

then the first term in Eq. (4.17) increases exponentially with time, and the bolometer overheats and burns up. If R_L is much greater than R_B and the thermal conductance does not change greatly with temperature, that is, $G \approx G_o$, then the unstable burnout condition is attained when

$$\alpha(T_1 - T_0) > 1. \tag{4.20}$$

For metals, in which α increases with temperature, the inequality described by Eq. (4.20) is not fulfilled and "self-burnout" does not occur. However, for semiconductors, self-burnout can occur at large bias currents. The inequality for self-burnout is

$$\frac{-b}{T_1^2}(T_1 - T_0) > 1. \tag{4.21}$$

Returning to the discussion of Eq. (4.17), it can be seen that under conditions in which the transient term goes to zero, the steady state solution of ΔT is

$$\Delta T = \frac{\eta\beta A_D P_o}{(G_e^{\,2} + \omega^2 C^2)^{1/2}}. \tag{4.22}$$

The change in bolometer resistance ΔR_B corresponding to the temperature change ΔT is, from the definition of α,

$$\Delta R_B = \alpha R_B \Delta T = \frac{\alpha R_B \eta b A_D P_o}{(G_e^{\,2} + \omega^2 C^2)^{1/2}}. \tag{4.23}$$

The signal voltage V_{R_L} appearing across the load resistor is

$$V_{R_L} = \frac{d(i_b R_L)}{dR_B}\Delta R_B = -\frac{V}{(R_B + R_L)} \cdot \frac{R_L \Delta R_B}{(R_B + R_L)}. \tag{4.24}$$

Assuming that $R_L >> R_B$, then the bias current i_b does not depend on R_B and ΔR_B. In that case, Eq. (4.24) becomes

$$V_{R_L} = i_b \Delta R_B. \tag{4.25}$$

Because the voltage V_{R_L} depends on ΔR_B and ΔR_B depends on the incident power P_o, V_{R_L} is the signal voltage, defined as V_s. Combining Eqs. (4.25) and (4.24) results in the expression for V_s

$$V_s = \frac{\alpha \beta \eta A_D i_b R_B P_o}{(G_e^{\,2} + \omega^2 C^2)^{1/2}}. \tag{4.26}$$

The responsivity $\Re$ is given by

$$\Re = \frac{V_s}{P_o A_D} = \frac{\alpha \beta \eta i_b R_B}{(G_e^{\,2} + \omega^2 C^2)^{1/2}}; \tag{4.27}$$

or

$$\Re = \frac{\alpha \beta \eta i_b R_B}{G_e (1 + \omega^2 \tau_e^{\,2})^{1/2}}; \tag{4.28}$$

where τ_e is defined as

$$\tau_e = \frac{C}{G_e}. \tag{4.29}$$

Here, τ_e is known as the "effective thermal response time." The dependence of G and τ on temperature due to bias current heating is termed the "electrothermal effect."

What is the importance of this? It is that G_e is the difference in two terms [see Eq. (4.16)]. The second term must be less than the first or G_e is negative and

the bolometer temperature increases exponentially with time, reaching burnout [see Eq. (4.19)]. Equations (4.20) and (4.21) show that this can happen with semiconductors but not with metals. As long as G_e remains positive, increasing the bias current I_b will increase the second term without changing the first. This will reduce the value of G_e, thereby increasing the signal voltage and the responsivity. On the other hand, as G_e decreases, the effective response time τ_e increases, which for some applications may be undesirable.

4.2.3 Case III: Joulean heating; pulsed bias

The greatest complexity occurs when the heat transfer equation includes the electrical bias (Joulean) heating and the heating due to the incident absorbed radiant power, but the electrical bias is pulsed rather than continuous. This is frequently the case when large focal plane bolometer arrays are employed. It turns out that the heat transfer equation then is nonlinear, and numerical solutions must be obtained, see Wood[2] and Jansson et al.[3] However, Wood[2] points out that if $\alpha(T_1 - T_0) << 1$, the dc bias equations (i.e., Case II above) and room temperature parameter values (i.e., ignoring the temperature dependence of the parameters due to Joulean heating) "produce numerical results that agree acceptably well—for many applications—with numerical calculations that take into account the full time dependence of the microbolometer parameters." Wood's Fig. 17, reproduced below as Fig. 4-3, provides an example of the results of a numerical calculation using the parameter values listed in his Table II, reproduced below as Table 4-1. The following quote is his description of the data.

> "As an example, Fig. 4-3 shows computed values of some microbolometer parameters, assuming the parameters summarized in Table 4-1 and assuming a net radiation power of 1 nW is absorbed within the microbolometer. The numerical calculations of Fig. 4-3 were performed using a BASIC program and an EXCEL™ spreadsheet, with 10 μsec time increments over an elapsed time of 30 msec, assuming a microbolometer initial temperature of 300 K: the time interval plotted in Fig. 4-3 covers only the last 200 μsec of the 30 msec period, at the end of which the second of two 100-μsec applied bias pulses is assumed to occur. The microbolometer temperature changes very rapidly during the bias pulse—at a rate of VI/C≈50,000°C per second. However, the 100-μsec duration of the bias pulse limits the total temperature increase to about 5°C. During the interval between bias pulses (30 msec) the microbolometer cools, and it reaches about 300.2 K—close to the substrate temperature (300 K)—by the time the next bias pulse begins. At any instant the effective G value is $G_e = P_o A_D / \Delta T$, where ΔT is the temperature perturbation caused by the presence of $P_o A_D$. This is computed and shown in Fig. 4-3. In the initial part of the time period plotted in Fig. 4-3, G_e is slightly greater than its assumed physical value of 1×10^{-7} W/deg K (Table 4-1), because insufficient time has elapsed (30

msec) for the microbolometer to reach the final equilibrium temperature expected from $P_o A_D$. The rapid decrease in G_e to values less than G during the bias pulse is due to the electrothermal effect. The time-dependent microbolometer responsivity is computed and shown in Fig. 4-3. The current responsivity $\Re_I = dI/dP_o A$ is plotted rather than the voltage responsivity $\Re_v$, because, in this example, the microbolometer is assumed to be operated at a constant voltage (R_L=0, Table 4-1) during a bias pulse."

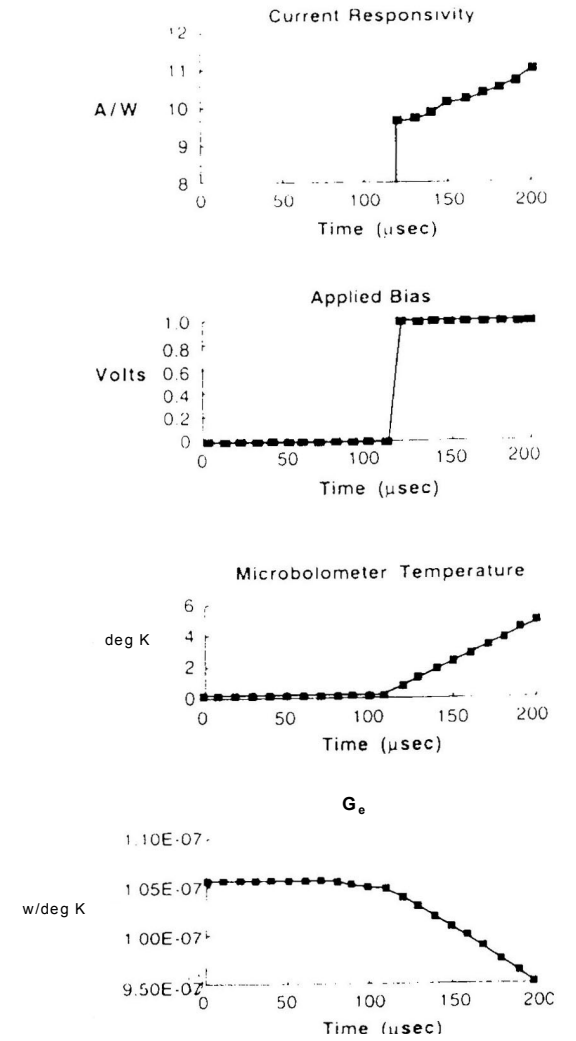

Figure 4-3. Numerical calculations made assuming the parameters in Table 4-1 as discussed in the text. G_e, effective value of thermal conductance of microbolometer to substrate. From R.A. Wood.[2]

Table 4-1. Assumed parameter values for Fig. 4-3. From R.A. Wood.[2]

Parameter	Value
$R(T_s)$	20 K Ω
R_L	0
V_b	1 V
Δt	100 μsec
$1/F$	30 msec
T_s	300 K
α	-0.02 K^{-1} at 300 K
C	1.0×10^{-9} J/deg K
G	1.0×10^{-7} W/deg K

4.3 Noise

There are four sources of noise in bolometers: Johnson noise, $1/f$ power law noise, temperature fluctuation noise, and background fluctuation noise. These four types of noise are uncorrelated; they add in quadrature, i.e., the total noise voltage is the square root of the sum of the squares of the noise voltages of the four sources. The magnitude of the noise voltage depends on the noise bandwidth. When using pulsed bias, an integrator is employed which limits the noise bandwidth to the frequency interval from 0 Hz to the reciprocal of the integration time, which is chosen to be equal to the pulse duration. In this way, the noise bandwidth B is given by

$$B = \frac{1}{2\Delta t}; \tag{4.30}$$

where Δt is the bias pulse duration.

The Johnson noise component of the total noise is given by V_J, where

$$V_J = (4kTR_B B)^{1/2}; \tag{4.31}$$

where k is Boltzmann's constant and, as before, T is the bolometer temperature, R_B is the bolometer resistance, and B is the bandwidth corresponding to the integration time.

The $1/f$ power law noise component is approximated by

$$V_{1/f} = (V^2 n / f)^{1/2}; \tag{4.32}$$

where

$$V = i_b R_B ; \tag{4.33}$$

f is the frequency at which the noise is measured, and n is the $1/f$ noise parameter. There is no accurate analytical expression for that parameter. Because $1/f$ power law noise decreases with increasing frequency, the integrated noise over the bandwidth B turns out to be

$$\int_B V_{1/f} df = V^2 n \ln\left(\frac{f_2}{f_1}\right). \tag{4.34}$$

Here f_2 is the upper frequency limit and f_1 is the lower frequency limit. Although $1/f$ power law noise is the dominant noise at low frequencies, it falls below Johnson noise at higher frequencies; the crossover is termed the "knee."

It turns out that for large focal plane arrays that are read out in a serial manner by pulsed bias, the bandwidth B [see Eq. (4.3)], can be sufficiently large that the Johnson noise over that bandwidth is much greater than the $1/f$ power law noise, provided that the $1/f$ power law noise parameter n is sufficiently small. This is true for the standard VOx material for which α=0.02/°C used in 240 × 320 pixel bolometer arrays operated at 30 Hz frame time, which are read out in the original Honeywell manner.[2]

In addition to Johnson noise and $1/f$ power law noise, a third form of noise is temperature fluctuation noise, V_{TF} (see Chapter 2). The mean square temperature fluctuations are given by

$$\overline{\Delta T_f^2} = \frac{4kT^2 B}{G(1+\omega^2\tau_T^2)^{1/2}} . \tag{2.25}$$

These temperature fluctuations cannot be distinguished by the readout mechanism from temperature changes caused by incident radiation that is absorbed by the pixel.

In many cases, the bandwidth B is large enough to include the $\omega\tau_T$ rolloff. In these cases, the mean square temperature fluctuations are given by Eq. (2.24).

$$\overline{\Delta T^2} = \frac{P_o}{4GC} . \tag{2.24}$$

Thus the mean square temperature fluctuation noise voltage is

$$\overline{V_{N,TF}^2} = \frac{4kTG\Re^2}{\eta} . \tag{4.35}$$

Similarly, the mean square background noise voltage is given by

$$\overline{V_{N,BF}^2} = 8A_D\eta\sigma k(T_D^{\,5} + T_B^{\,5})\Re^2 . \tag{4.36}$$

Here T_D and T_B are the pixel temperature and the background temperature. The field of view is assumed to be 2π steradians.

The total mean square noise voltage is obtained by adding together the four contributions

$$\overline{V_{N,Tot}^2} = \overline{V_{N,J}^2} + \overline{V_{N,1/f}^2} + \overline{V_{N,TF}^2} + \overline{V_{N,BF}^2} . \tag{4.37}$$

4.4 Noise Equivalent Temperature Difference

The NETD is determined by inserting $\left[\overline{\left(V_{N,\mathrm{Tot}}^2\right)}\right]^{1/2}$ for V_N in the NETD expression, employing the appropriate expressions for the responsivity $\Re$ from Cases I, II, and III. The NETD is given by

$$\mathrm{NETD} = \frac{4F^2 V_N}{\tau_o A_D \Re(\Delta P/\Delta T)_{\lambda_1-\lambda_2}}; \tag{1.6}$$

where V_N is the total noise voltage over the array readout electrical bandwidth, τ_o is the transmittance of the optics, and $(\Delta P/\Delta T)_{\lambda_1-\lambda_2}$ is the change with respect to temperature of the power per unit area emitted by a blackbody at temperature T, measured within the spectral bandwidth between λ_1 and λ_2. For λ_1=8 μm, λ_2=14 μm, and T=295 K, the value for $(\Delta P/\Delta T)_{8-14}$ is 2.62×10^{-4} W/cm^2 deg K. F is given by

$$F = \frac{1}{2\sin\theta}; \tag{1.7}$$

where θ is the half angle of the cone of convergence of radiation focused by the optics to the focal point where the array is located.

In practice, assumptions are made about the noise in order to reduce the complexity. The Johnson noise is always included. For Cases I and II in which the bias is constant, 1/*f* power law noise should be included. For Case III, pulsed bias, the readout electrical bandwidth is large; in practice it turns out that 1/*f* power law noise is limited to low frequencies, so that the Johnson noise may exceed 1/*f* power law noise over the bandwidth. Temperature fluctuation noise is included in all cases. As of this writing, background fluctuation noise has not yet been of consequence; that will change as the technology matures.

4.5 Choice of Resistive Materials

4.5.1 Vanadium oxide

The standard resistive material has been vanadium oxide, VOx, made by sputtering a thin film of the mixed oxides on a Si_3N_4 microbridge substrate. The material was developed originally at Honeywell, see Wood.[2] The temperature coefficient of resistance (TCR) versus resistivity is shown in Fig. 4-4. Figure 4-5 illustrates the resistance as a function of temperature for a typical VOx thin film.

The temperature coefficient of resistance, α, is usually quoted as -0.020/°C (2%/°C), yet it can be seen from Fig. 4-4 that higher values can be attained. There are two reasons for not using compositions (x-values) with substantially higher temperature coefficients. First, the scatter in the data shows that reproducibility of properties suffers in the higher x-value films. Second, i^2R heating becomes a problem with high resistivity films. This exacerbates the nonlinear temperature versus time problem during the pulse duration, see Wood.[2]

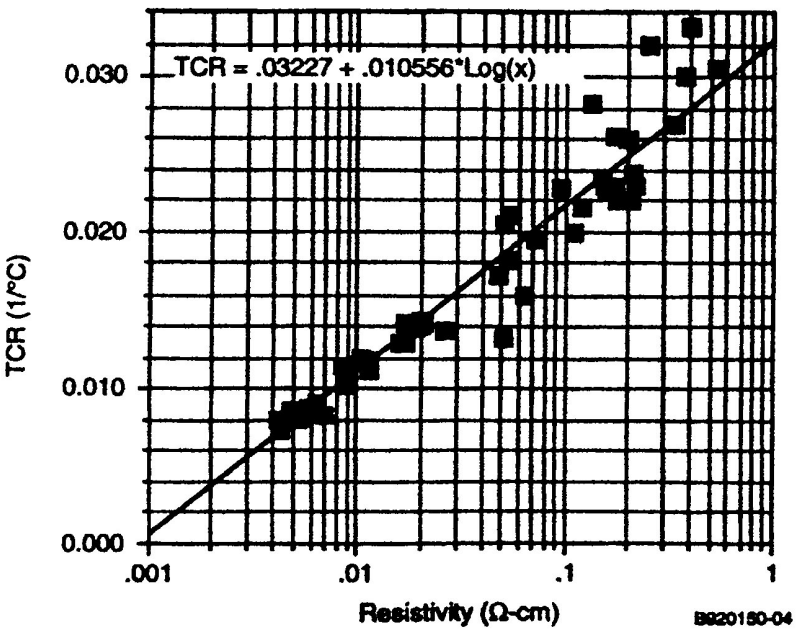

Figure 4-4. Temperature coefficient of resistance (TCR) versus resistivity for thin films of mixed vanadium oxides. From R.A. Wood.[2]

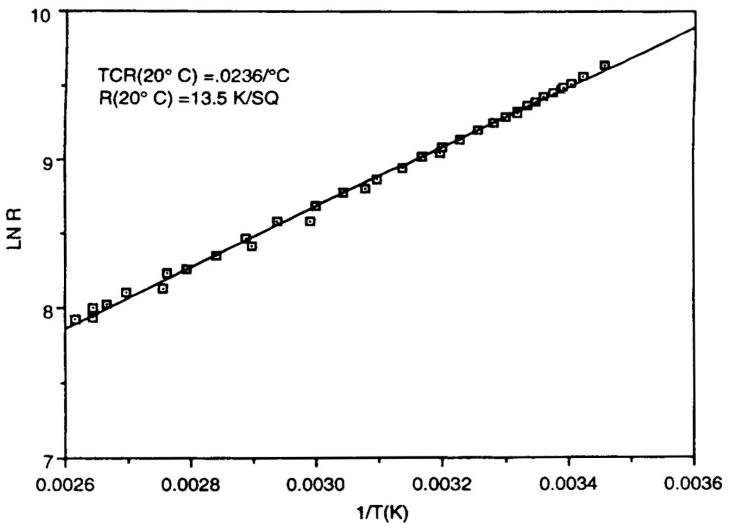

Figure 4-5. Resistance versus temperature for thin films of mixed vanadium oxides. From R.A. Wood.[2]

4.5.2 Amorphous silicon

Thin-film bolometers based on the use of amorphous silicon (a-Si) have been investigated for at least 15 years. Liddiard[4] has reported room temperature TCR values ranging from $-0.025°C^{-1}$ for doped, low resistivity films to $-0.08°C^{-1}$ for high resistivity materials. Tissot[5] illustrates the relationship between the TCR and the resistivity of a-Si, see Fig. 4-6.

Although high TCR values are attainable, e.g., $-0.08°C^{-1}$, they are accompanied by "an unacceptable level of $1/f$ noise" according to Liddiard.[4] This is not surprising, given the high resistivity of the films. The properties of the films depend upon the method of preparation and the type of dopant, e.g., hydrogen, such films being designated a-Si:H. Non-hydrogenated amorphous silicon films have been prepared with room temperature resistivities in the 500–1000 ohm cm range, but the TCR was about $-0.02°C^{-1}$. Amorphous silicon can be deposited by photo-enhanced chemical vapor deposition (PECVD), a process that is compatible with epitaxy.[6]

Because the typical resistivity of amorphous silicon films is several orders of magnitude higher than that of VOx, a-Si finds application in uncooled arrays in which the bias is continuous rather than pulsed. That is because the signal in bolometers depends on $i_b \alpha R$. where i_b is the bias current, whereas the power dissipation, which causes the rise in pixel temperature, depends on $i_b^2 R$. This is, of course, an oversimplified argument, because pulsed bias is on a given pixel for a very short time, typically a few microseconds, whereas continuous bias is always on each pixel. Nevertheless, design tradeoffs dictate some advantage for a-Si in certain instances.

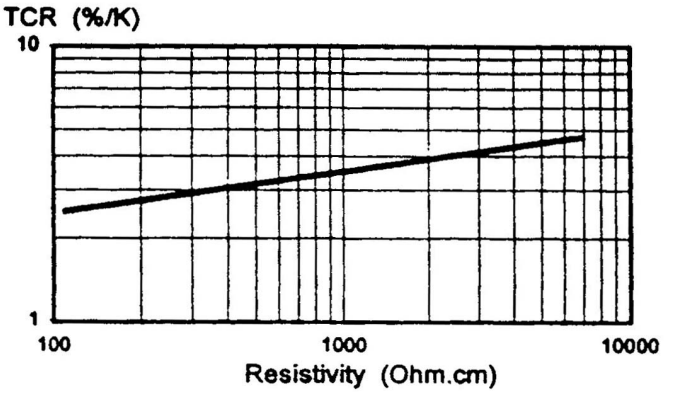

Figure 4-6. Evolution of the TCR as a function of the electrical resistivity of a-Si. From Tissot.[5]

4.5.3 Thermistor materials

Thermistor (from "thermally sensitive resistor") materials first developed at Bell Laboratories during World War II, are oxides of manganese, cobalt, and nickel that crystallize in the spinel structure. They are semiconductors that exhibit negative temperature coefficient of resistance. Single pixel thermistor bolometers have been commercially available for about 50 years. The principal material investigated is $(MnNiCO)_3O_4$, which has a negative temperature coefficient of resistance of about $0.04°C^{-1}$ at room temperature, and a bulk resistivity of 250 ohm cm.[7]

Because they exhibit a large amount of $1/f$ power law noise arising at grain boundaries, thermistor thin films have not been found to be useful in uncooled bolometer thermal imaging arrays.

4.5.4 Titanium

Titanium (Ti) is a metal that in thin film form has a temperature coefficient of resistance of 0.004°C. Although low values of $1/f$ power law noise are found, its very low temperature coefficient of resistance causes it to be of little use in uncooled bolometer arrays.

4.5.5 P-N junction diodes

Mitsubishi Electric Corp. has developed an uncooled bolometer array in which the "resistive" material is actually a p-n junction diode that is forward biased. The diodes are deposited in thin film form on silicon-on-insulator thin films. The diodes have low $1/f$ power law noise. A 320×240-pixel array has been reported.[8] Low manufacturing cost is said to be a principal advantage.

References

1. P. W. Kruse, L. D. McGlauchlin, and R. B. McQuistan, *Elements of Infrared Technology*, pp. 345-349, John Wiley and Sons, Inc., New York (1962).
2. R.A. Wood, "Monolithic silicon microbolometer arrays," Chapter 3 of *Uncooled Infrared Imaging Arrays and Systems*, *Semiconductors and Semimetals 47*, P. W. Kruse and D. D. Skatrud, eds., Academic Press, San Diego (1997).
3. C. Jansson, U. Ringh, and K. Liddiard, "Theoretical analysis of pulse bias heating of resistance bolometer infrared detectors and effectiveness of bias compensation," Proc. SPIE Vol. 2552, p. 644 (1995).
4. K.C. Liddiard et al., "Progress of Swedish-Australian research collaboration on uncooled smart IR sensors," Proc. SPIE Vol. 3436, *Infrared Technology and Applications XXIV*, p. 478 (1998).
5. J-L Tissot et al., "LETI/LIR's amorphous silicon uncooled microbolometer development," Proc. SPIE Vol. 3379, *Infrared Detectors and Focal Plane Arrays III* (1994).
6. J.F. Brady, "Advances in amorphous silicon uncooled IR systems," Proc. SPIE Vol. 3698, *Infrared Technology and Applications XXV*, p. 161 (1999).
7. R. Dannenberg, A. Doctor, and S. Baliga, "Electrical and optical properties of $Mn_{1.56}CO_{0.96}Ni_{0.48}O_4$, Proc. SPIE Vol. 3379, p. 16 (1998).
8. T. Ishikawa et al., "Low-cost 320×240 uncooled IRFPA using conventional silicon IC process, Proc. SPIE Vol. 3698, *Infrared Technology and Applications XXV*, p. 556 (1999).